Life Science Informatics Publications
Research Journal of Life Sciences, Bioinformatics, Pharmaceutical and Chemical Sciences
Journal Home page http://www.rjlbpcs.com/
RJLBPCS
ISSN 2454-6348

Original Research Article **DOI: 10.26479/2019.0502.78**

COMPUTATIONAL STUDIES TO DECIPHER THE PLAUSIBLE INHIBITION OF TYPE III SECRETION SYSTEM (T3SS) ATPases INVOLVED IN BACTERIAL MOTILITY AND VIRULENCE

Jagadeesh Kumar D*, Sneha Paturi, Kiran chandrika S, Ashwathi P, Priya Narayan, Nagendra H G

Department of Biotechnology, Sir M. Visvesvaraya Institute of Technology, Bangalore, India.

ABSTRACT: Flagella are filamentous organelles that facilitate bacterial locomotion, recognized to have multiple roles like adhesion to the host, biofilm formation, penetration into mucosal layer and invasion of epithelial cells. The proteins present in the flagella are prime factors dictating the pathogenicity of the organism. Therefore it will be interesting to study the structure, regulation and functionality of these proteins, in order to explore and design inhibitors, which could aid in controlling the virulence and pathogenicity of flagellates. In our study, 17 proteins that are conserved and part of bacterial mobility, across the pathogens viz., *Salmonella typhimurium, Campylobacter jejuni, Helicobacter pylori, Escherichia coli, Vibrio cholera, Psuedomonas aeruginosa and Clostridium botulinum* have been considered for a detailed *In silico* analysis. Our work focuses upon the plausible inhibition of FliI ATPase (Flagella ATP synthase), which are the most important T3SS of the export apparatus crucial for bacterial motility. Its comparison with mitochondrial ATPase, and single ATPase, YscN, an Injectosome component necessary for delivery of virulence factors, are also conducted. The Natural compounds and antibiotics have been screened via binding studies, based upon the strength of interactions across different pockets of FliI ATPase, for their potential use as therapeutic agents towards confronting pathogenicity.

KEYWORDS: Flagella; Motility; T3SS; Docking; FliI ATPase.

Corresponding Author: Dr. Jagadeesh Kumar D* Ph.D.
Department of Biotechnology, Sir M. Visvesvaraya Institute of Technology, Bangalore, India.
Email Address: jk4you@gmail.com

1. INTRODUCTION

Flagella are locomotive organelles, which are extremely conserved across bacterial species [1] that allow the microbes to move towards favorable environments. Several studies on flagella have revealed that besides having a locomotive function, it also plays crucial roles in adhesion, biofilm formation, colonization and bacterial pathogenicity [1, 2, 3, 4]. The flagellum is made up of nearly 50 proteins and primarily consists of three parts: The basal body which acts as a rotary motor, hook which functions as the universal joint and a filament that works as a helical propeller [5] [Figure 1]. Some components of flagella apparatus are common to the most bacterial species, but significant deviations are also rarely observed [6]. The study of various proteins throws light into the evolutionary history of this notable organelle [7, 8]. The expression of the components of the flagella at the appropriate time and within correct environment is controlled by a very complex and remarkable regulatory system [9]. The flagellar export apparatus plays a decisive task in the transport of diverse components for its assembly. It is a T3SS (Type 3 Secretion System) which is widespread among Gram-negative bacteria and recognized to be of two kinds of T3SS: one involved in flagellar motility (F-T3SS) and a second type, Non-flagellar T3SS (NF-T3SS) called Injectisome. This needle-like complex is used by disease-causing bacteria to punch holes in the host's target cells and helps in the secretion of bacterial virulence Proteins from bacterial cytoplasm across the eukaryotic host cells, a trait frequently associated with virulence [10]. The basal body proteins within the inner membrane are highly conserved in all T3SS, including Injectosomes and flagellar systems. [11]. The flagellar-T3SS and NF-T3SS systems contain proteins that share a high degree of homology, signifying an evolutionary correlation from a bacterial flagellum ancestor [9]. These proteins include ATPase complex structures, containing six Integral membrane and 15 to 20 membrane-associated proteins which constitute the type III secretion apparatus. [12]. Flagellar-T3SS consists of three soluble proteins (FliH, FliI and FliJ) and six integral membrane proteins (FlhA, FlhB, FliO, FliP, FliQ and FliR) that interacts with the chaperones (FliS, FliT, FlgN) along with FliK that acts as hook length control protein and is believed to be located at the base of the flagellum [13, 5]. The export path diameter is only 2nm which requires flagellar proteins to be largely unfolded for entry into and translocation through the central channel [14, 15] [Figure 1]. Biofilm formation, adhesion, chemotaxis and modification of the immune system are additional functions of this nanomotor [13, 16]. A component of the motor-switch complex of the flagellar basal body is encoded by the protein fliG leading to bacterial invasiveness. Biofilm formation is important for pathogen survival which is mediated by flagellar motility [17]. Upon bacterial colonization, virulence factors can be exported by the flagellar secretion system [18]. FliI is the peripheral membrane ATPase crucial to the type III protein export mechanism required for the assembly of the bacterial flagellum. FliI ring structure has six-fold symmetry and an external diameter of approximately 10 nm. The oligomeric ring has a central cavity of 2.5-3.0 nm, which is

comparable to the known diameter of the flagellar export channel into which export substrates feed. The soluble export component FliI is an ATPase and converts chemical energy released by ATP hydrolysis into mechanical work which is critical for the export. [Figure 2]. FliH and FliJ form a complex with this and guide the export substrates from the cytoplasm to the export gate complex, comprising of 6 membrane proteins [19].

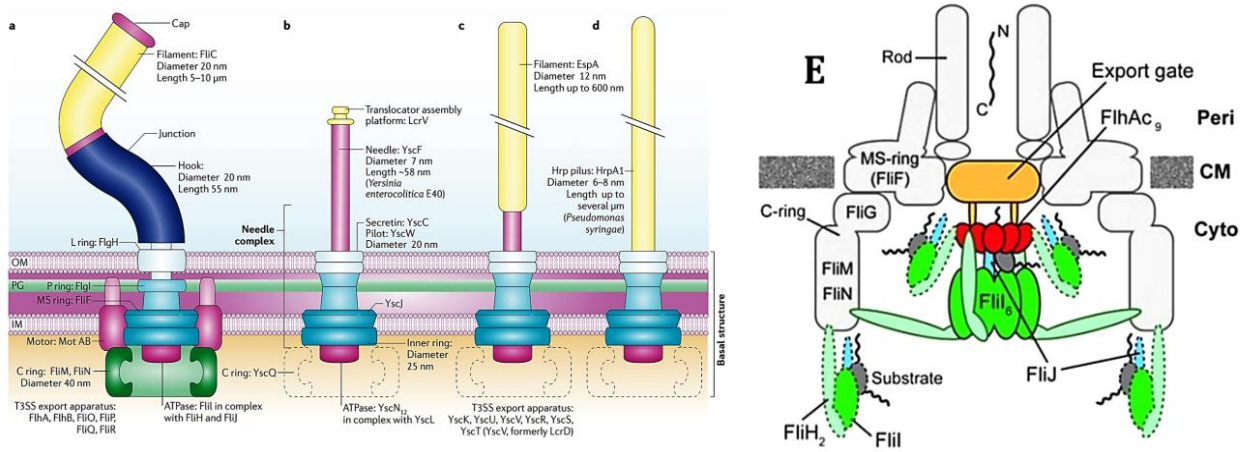

Figure 1: Structure of the flagellum and the injectisomes. Schematic representation of the flagellum (a) Yscinjectisome. (b) injectisome from EPECs. (c) and the injectisome from plant pathogens. (d) For the injectisomes, the C ring is represented by a dashed line as information on this component is still scarce. IM, inner membrane; OM, outer membrane; PG, peptidoglycan. [Figure adopted from: Cornelis GR. The type III secretion injectisome] Nat Rev Microbiol. 2006 Nov; 4(11):811-25. (E): Schematic diagram of the bacterial flagellar export apparatus: showing the proteins involved in the export gate. [Figure is adopted from: Fan Bai et.al Scientific Reports 4, Article number: 6528 (2014)].

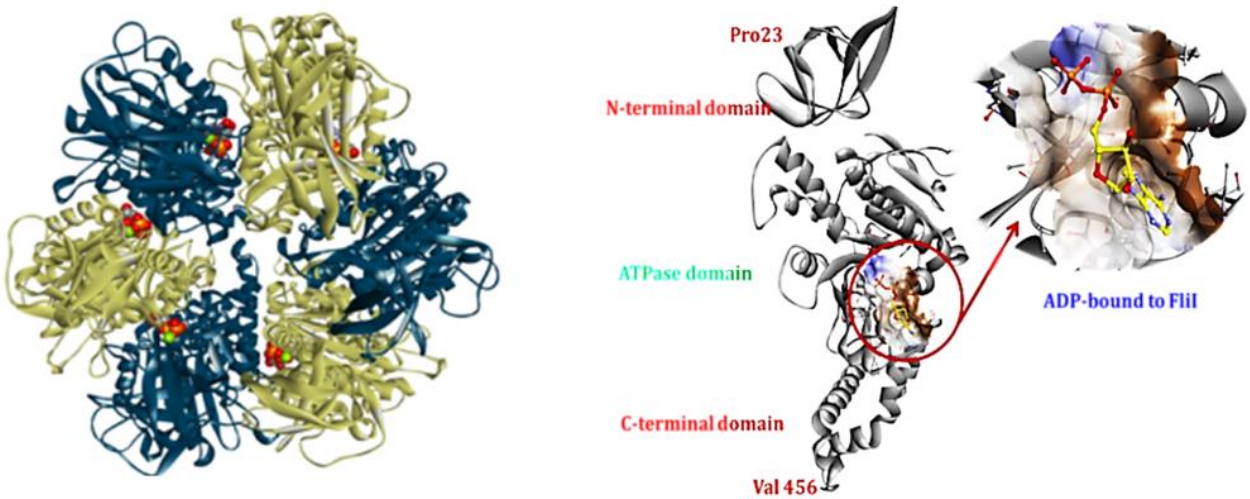

Figure 2: A. Stereo view of the ribbon diagram of FliI hexamer model B. Structure of FliI ATPase, FliI, PDB ID: 2dpy (B chain) Close-up stereo view of the ADP nucleotide-binding site. Organism: Salmonella enterica Crystal Structure of the flagellar type III ATPase FliI, PDB ID: 2dpy (B chain)

FliI, a component of the flagellar export apparatus with sequence similarity to the catalytic β subunit of the bacterial F0F1 ATPase [1] undergoes multimerization which is promoted by the presence of bacterial phospholipids. Soluble FliI exists as a monomer (≈49kDa) but FliI oligomerises in presence of ATP, shows 6 fold symmetry with external diameter of 10nm and with central cavity of 2.5-3nm which is also the diameter for the export channel [13]. It lacks transmembrane domains and behaves as peripheral protein [15, 20]. Likewise, the pathogens also use a type III secretion system (T3SS) Injectisome nanomachine to deliver virulence factors directly from bacterium into host mammalian cells. This involves a single ATPase, YscN, necessary for delivery of virulence factors and share significant similarity with FliI ATPase. It is known form the early genetics studies that, apart from *FliI* ATPase, a core of 15 proteins from the injectisome share significant similarities with components of the flagellum [14, 22]. Therefore, it is understood from the above knowledge that, both the ATPases, FliI and YscN, plays a significant role delivery of virulence factors [15, 21]. Thus, in view of the scenario of resistance to the current antibiotics, discovery of new compounds from natural products with antimicrobial activity is the dire need of hour. Therefore, this study is aimed at screening natural compounds as potential antibiotics, from the class which are known to possess defined antimicrobial properties. Exploring their interactions with the ATPases that are responsible for the bacterial motility and virulence, this work would offer clues as leads molecules for tackling pathogenicity and antimicrobial resistance.

2. MATERIALS AND METHODS

Our Computational study focuses on type III secretion system (T3SS) ATPases as preferred targets for development of novel antibacterial therapeutics. The preliminary work involved the documentation of pathogenic bacteria with flagella through extensive literature survey form PUBMED [25]. The exploration of different parts of flagella, its proteins components, and their location were investigated to understand its morphology and function. A total of 44 proteins and their sequences from Universal Protein Resource- Uniprot [26] were retrieved. Amongst them, only 17 proteins were found to have structural details as recorded in the Protein Databank (PDB) [27]. [Table1]. 18 proteins that are commonly present across the flagella were however without defined structural details, and these are illustrated in table 2. The other 9 proteins are specific to select organisms only, and hence were deleted from the study. The methodology followed in this investigation is depicted as a flow chart in Figure-7. For our analysis, only 17 proteins which possessed structural information were subjected to extensive sequence and structural studies. Key proteins responsible for flagellar motility were evaluated and considered for further analysis. The protein FliI (Flagella ATP synthase) was specifically selected for an in-detail analysis, since this type three secretion system (T3SSs) is required by dozens of pathogens, including the causative agents of plague, typhoid fever, pneumonia etc.

Table 1: Details of Flagellar proteins with defined structures

SL NO	PROTEIN	ORGANISM	UNIPROT ID	LENGTH	PDBID	DESCRIPTION	LIGAND	PMID
1	FlgL	*S. typhimurium*	P16326	317	2D4X	Flagellar hook-associated protein 3	–	–
2	FliK	*S. typhimurium*	P26416	405	2RRL	Flagellar hook-length control protein Hook is built by FlgE secretion. FliK is the "hook length regulatory" protein.	–	21510958
3	FliI	*S. typhimurium*	P26465	456	2DPY	Flagellum-specific ATP synthase	ADP	17202259
4	FlhD	*E coli*	P0A8S9	116	1G8E	Flagellar transcriptional regulator	–	11169099
5	FlhB	*S. typhimurium*	P40727	383	3B0Z	Flagellar biosynthetic protein FlhB Regulates FlgE and FliK can be secreted.	Na+, Zn2+	23633590
6	FlgA	*S. typhimurium*	P40131	219	3TEE	Flagella basal body P-ring formation protein FlgA	Cl⁻ ion, glycerol	–
7	FlhA	*S. typhimurium*	P40729	692	3A5I	Flagellar biosynthesis protein FlhA	–	20199603
8	FlgK	*S. typhimurium*	P0A1J5	553	2D4Y	Flagellar hook-associated protein 1	–	–
9	FliS	*H.pylori*	O25448	126	3IQC	Flagellar protein	–	–
10	FliM	*H.pylori*	O25675	354	4GC8	Flagellar motor switch protein	–	23614777
11	FliJ	*S. typhimurium*	P0A1K1	147	3AJW	Flagellar FliJ protein	Hg2+	21278755
12	FliT	*S. typhimurium*	P0A1N2	122	3A7M	Flagellar protein	–	20421493
13	FliG	*H.pylori*	O25119	343	3USW	Flagellar motor switch protein	–	22325779
14	FlgE	*S. typhimurium*	P0A1J1	403	1WLG	Flagellar hook protein	–	15510139
15	MotB	*H.pylori*	P56427	257	3SOY	Motility protein	SO4-	22120737
16	FlgD	*P.aeruginosa*	Q9I4Q0	237	3OSV	Flagellar basal-body rod modification protein	Glycerol	–
17	CheY	*Vibrio cholerae*	Q6BBK8	130	4HNS	CheY homolog	Mg ion, BeF3ion	24066084

Table 2: Flagellar proteins without structures

- C ring proteins: FliG, FliN
- Hook proteins: FlgE, FliK, FlgD
- Flagella Basal Body Proteins: FliE, FlgB, MotA, MotB, FlgC, FlgF
- Export apparatus: FliH, FliI, FliO, FliP, FliQ, FliR, FliJ, FLhB,
- FLhA, CheY
- L ring : FlgH
- P ring : FlgI
- MS ring protein: FliF
- Filament proteins: FliC, FliD
- H-F junction: FlgL, FlgK, FlgM

SL NO.	PROTEIN	ORGANISM	UNIPROT ID	LENGTH	DESCRIPTION
1	FliN	*E.coli*	P15070,	137	Flagellar motor switch protein
2	FliP	*Clostridium botulinum*	A5I582	258	Flagellar biosynthetic protein
3	FliD	*Campylobacter jejuni*	Q5HVL8	636	Flagellar hook associated protein
4	FlgC	*Clostridium botulinum*	A5I598	144	Flagellar basal body rod protein
5	FlgF	*Vibrio cholerae serotype 01*	A5F680	249	Flagellar basal body rod protein
6	FlgM	*S. typhimurium*	P26477	97	Negative regulator of flagellin synthesis
7	FlgG	*Treponema pallidum*	O83926	264	Flagellar basal body rod protein
8	FliE	*E.coli*	P0A8T5	114	Flagellar basal body complex protein
9	FliF	*Chlamydia trachomatis*	G4NNR2	334	Flagellar M-ring protein
10	FliC	*S.typhimurium*	P06179	495	Flagellin
11	FliH	*Treponema pallidum*	O83416	309	Flagellar assembly protein
12	FliO	*Pseudomonas aeruginosa*	Q51467	150	Flagellar protein
13	MotA	*E.coli*	P09348	295	Motility protein A
14	FlgB	*S.typhimurium*	P16437	138	Flagellar basal body rod protein
15	FliQ	*Clostridium botulinum*	A5I581	89	Flagellar biosynthetic protein
16	FliR	*Treponema pallidum*	P74932	265	Flagellar biosynthetic protein
17	FlgH	*E.coli*	P0A6S0	232	Flagellar L-ring protein
18	FlgI	*E.coli*	P0A6S3	365	Flagellar P-ring protein

The X-ray crystal coordinates of the FliI protein were downloaded in pdb file format from the Research Collaboratory for Structural Biology Protein Data Bank (http://www.rcsb.org, deposition number 2DPY). The

energy minimization on the FliI was conducted to relieve any highly unfavorable atomic clashes and to converge the molecule to its lowest-energy conformation. Likewise, single ATPase, YscN an Injectosme component necessary for delivery of virulence factors was also evaluated. Atomic coordinates for Natural inhibitors and antibiotics as shown in table 10 & 11 were collected from PubChem Compound Database (PUBCHEM) website (https://pubchem.ncbi.nlm.nih.gov/) [28]. Selected ligands were docked across ATP binding domains of the protein FliI, in order to screen for suitable molecules that could exhibit competitive inhibition. Docking studies were carried out using FlexX [29] and Discovery studio 3.5 [30].

Figure 7: Flowchart showing the various methods used in the Study

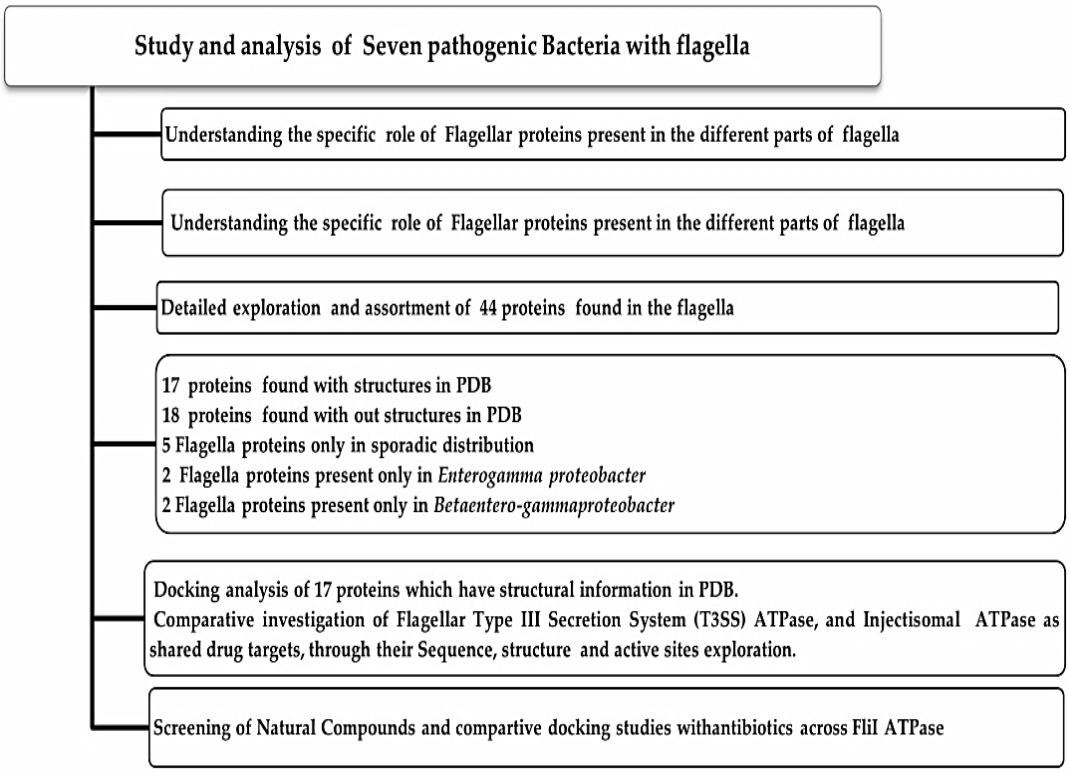

3. RESULTS AND DISCUSSION

Our preliminary structural study involved examination of ≈44 different proteins associated with the formation of flagella apparatus. The role of each protein was analyzed and tabulated in the Table 1 & 2. The verified 17 proteins with structures were retrieved from PDB and analyzed for the presence of ligands, as none of these 17 proteins were defined with any ligands/ inhibitors. Further, Comprehensive exploration of Flagellar basal body structure reveals approximately about 20 proteins required forming the flagellar basal body; about half these proteins have clear counterparts in the injectisome which are shown in the table 3. Likewise, it is predicted from the study that, FliH, FliI, and FliJ of the flagellar T3SS system are believed to assist delivery and unfolding of secretion substrates to the export apparatus and to the Motility of the flagella. Thus, this assisted us to know the key proteins involved in the flagellar T3S system and to further explore the detailed sequence

and structural correlations of FliI ATPase [Figure 2].

Table 3: Flagellar Proteins with their counterparts in the injectisome

Sl No	Flagellum (*S. enterica*)	Injectisome (*S. enterica* SPI-1)	Injectisome (*Yersinia* ssp. Ysc)	Injectisome (*Shigella* ssp.)	Injectisome (enteropathogenic *Escherichia coli* EPEC)	Structure/Function
1.	FliF	PrgH/PrgK	YscJ	MxiJ	MxiJ	MS-ring inner-membrane ring
2.	FliI	InvC	YscN	Spa47	EscN	ATPase
3.	FliJ	-	YscO	-	-	T3S chaperone
4.	FliGMN	PrgJ/SpÅ	YscQ	Spa33	-	C-ring cytoplasmic ring (HrcQ in Pseudomonas)
5.	FliP	SpaP	YscR	Spa24	-	T3S apparatus inner-membrane protein
6.	FliQ	SpaQ	YscS	Spa33	-	T3S apparatus inner-membrane protein
7.	FliR	SpaR	YscT	Spa29	-	T3S apparatus inner-membrane protein
8.	FlhA	InvA	YscV	MxiA	-	T3S apparatus inner-membrane protein
9.	FlhB	SpaS	YscU	Spa40	-	T3S apparatus inner-membrane protein
10.	N/A	InvG	YscC	MxiD	-	outer-membrane ring
11.	FlgE	PrgI	YscF	MxiH	EscF	extracellular needle
12.	N/A	SipBC	YopBD	IpaBC	EsoBD	translocation pore
13.	FliC	SseB	LcrV	IpaD	EspA	needle extension
14.	FliH	-	YscL	MxiN	-	ATPase regulator
15.	FliK	InvJ	YscP	Spa32	-	hook/needle length regulator

3.1

Sequence and Structural Comparison between FLiI, YsCN & F1 ATPase.

In order to appreciate the conservation and diversity among F1 ATPase of bovine mitochondria, Flagellum-specific FLiI and Injectosome specific YsCN ATP synthase, pairwise alignments were carried out. The results reveals that the T3SS ATPases share below 23% amino acid sequence identity with F1 ATPase from bovine mitochondria, however, very well conserved with T3SS ATPases across difference species. Percentage of identify and similarity are highlighted in Table 4. Likewise the α and β subunits of F1 ATPase from bovine mitochondria (PDB ID code: 1BMF) are superimposed onto FliI (PDB ID code: 2DPY) to understand the ADP binding and active site similarity. Structure-based sequence alignment was also carried out across FliI and YscN members of the T3SS cytoplasmic ATpases proteins. The alignment (Fig. 3 A & C) revealed extensive structural homologies and novel ATP binding structural motifs. The residues that are highly conserved between FliI from *S. typhimurium* and YscN-*Yersinia spp. Ysc* is highlighted in red. Red boxes indicate the nucleotide binding residues and blue box shows residues forming a hydrophobic pocket consisting of amino acids Val-190, Met-194, Tyr-363, Pro-364, and Ile-436. [Refer Figure 3 A-D], indicating the conserved through the bacterial bacterial ATPases. The conserved P-loop is also shown by the red Box.

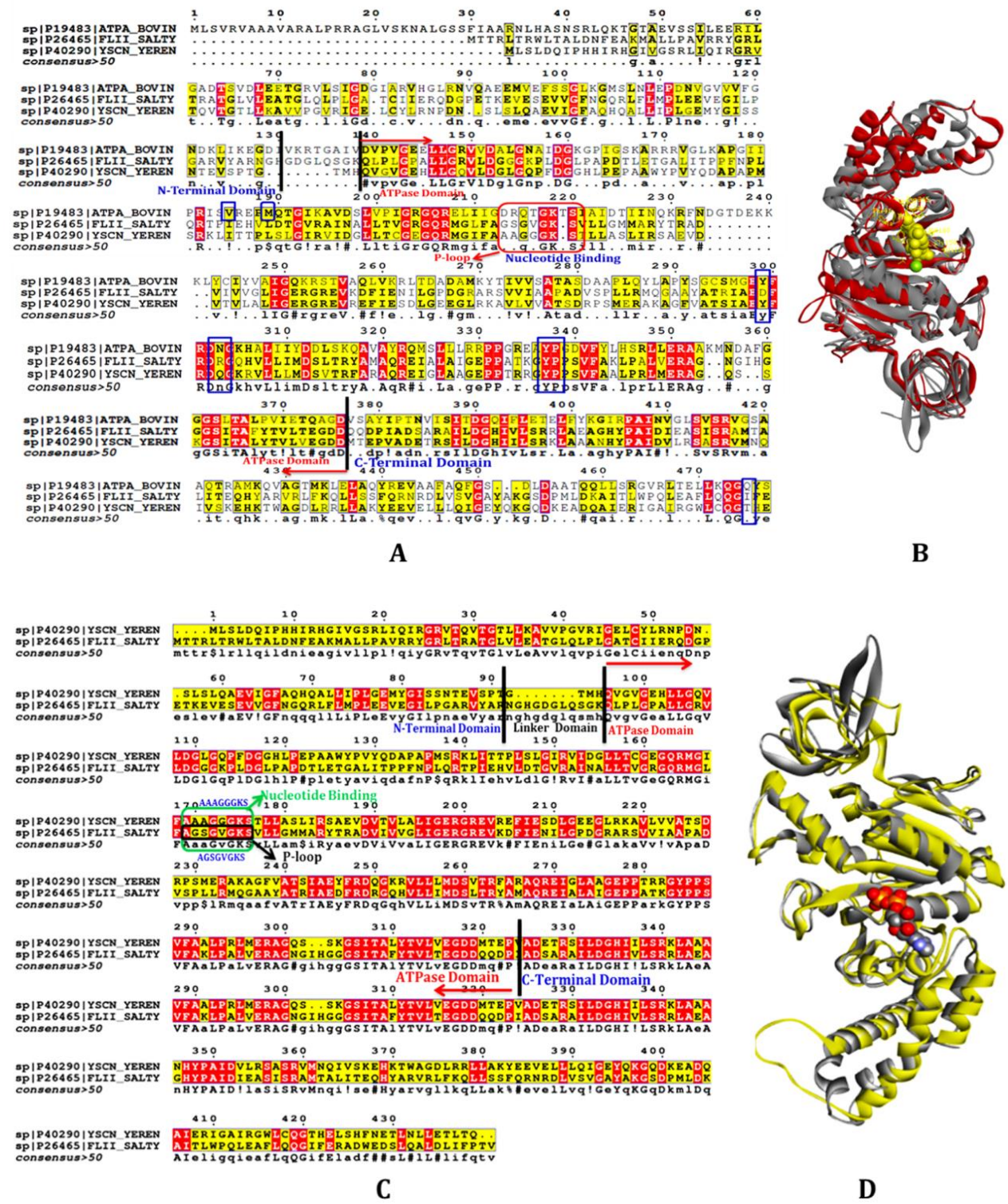

Figure 3: A] Sequence alignment of flagellar type III ATPase ATPA_BOVIN, FliI and ATP synthase YscN. N-terminal ATPase domain and C-terminal domain are shown. The P loop is shown by the red Box. The residues conserved between F1 ATPase of bovine mitochondria, FliI from S. typhimurium and YscN-Yersinia spp. are highlighted in red. Red boxes indicate the residues nucleotide binding and blue box shows residues forming a hydrophobic pocket-Val-190, Met-194, Tyr-363, Pro-364, and Ile-436. B] Structural Overly of flagellar type III ATPase ATPA_BOVIN, FliI and ATP synthase YscN. C] Sequence alignment of flagellar type III ATPase FliI and YscN ATP synthase. The Conserved Nucleotide binding amino acid residues are highlighted as green Box and red arrow line. Similarly, Blue boxes highlight the inhibitor binding sites, used in the present study. The sequence similarities between the

flagellum ATPase and the injectisome YscN ATPase suggest an evolutional origin shared by these molecular machines. D] Structural Overly of Sequence alignment of flagellar type III ATPase FliI and ATP synthase YscN

Table 4: Showing the Percentage Identity, similarity, I* represents Identity, #S denotes Similarity, with sequence of ATPase's of ATP synthase subunit beta, mitochondrial (Bovine) with Flagellum-specific ATP synthase with Probable ATP synthase YscN, Probable ATP synthase PAL_SALTY, and Probable ATP synthase SPAL_SHIFL. The bacterial enzymes have less than 23% identity to human ATPases and the active sites show significant differences between bacterial and human enzymes.

ATPase Name and Uniprot ID	ATPA_BOVIN	FLII_SALTY	YSCN_YEREN	PAL_SALTY
Mitochondrial membrane ATP synthase ATPA_BOVIN (P00829) Bos taurus (Bovine)	-	-	-	-
Flagellum-specific ATP synthase FLII_SALTY (P26465) *Salmonella typhimurium*	*I 133/595-(22.4%) #S 215/595 (36.1%)	-	-	-
Probable ATP synthase YscN YSCN_YEREN (P40291) *Yersinia pseudotuberculosis serotype I*	*I 123/607 (20.3%) #S 197/607 (32.5%)	*I 191/468 (40.8%) #S 269/468 (57.5%)	-	-
Probable ATP synthase SpaL PAL_SALTY-(P0A1B9) *Salmonella typhimurium*	*I 112/577 (19.4%) #S 99/577(34.5%)	*I 170/464(36.6%) S # 258/464 (55.6%)	*I 196/449 43.7%) #S 278/449 (61.9%)	-
Probable ATP synthase SpaL SPAL_SHIFL (P0A1C1) *Shigella flexneri*	*I 122/568 (21.5%) S # 198/568 34.9%)	*I 176/470 (37.4%) #S 251/470 (53.4%)	*I 196/449 (43.7%) #S 278/449 (61.9%)	*I 243/434 (56.0%) #S 318/434 (73.3%)

3.2.

Structural Similarity between FliI and F_1-ATPase Subunits

To understand the structural similarity, fold and deviations in ATP binding site, Molecular superimposition and Root-mean-square deviations (RMSD) procedures were carried out between three different α and β subunit structures of Hetero-hexamer structure of bovine mitochondrial F1-ATPase α/β subunits [PDB ID- 1BMF] and similarly with FliI [PDB ID- 2DPY] by using Discovery studio 3.5 tools. Superposition of the Molecules is presented in the figure 4, and RMSD obtained across Cα atoms of α and β subunits are tabulated in table 5. From the table, RMSD values discloses that, αABC subunits values ranges from 0.70 Å -1.02 Å, while αA and αB chains showed the least value of 0.70Å, indicating high similarity between them. While, βDEF subunits show RMSD value of 0.59Å, signifying the high similarity among DEF Subunits. Similarly, RMSD was calculated by superimposing FliI ATPase domain (A chain-PDB ID- 2DPY) with F1- ATPase subunits (αABC & βDEF). Results from the table reveal that, RMSD values ranges from 1.40~1.51 Å across αABC and 1.70~1.78Å over αDEF subunits, specifying that FliI ATPase and bovine mitochondrial F1-ATPase α/β subunits exhibit prominent structural similarity. Similarly, The active site residue RMSD (Table 6) calculated to find out the similarity in ADP binding region. The C alpha RMSD values range from 0.46 Å to 1.71 Å and All atoms RMSD 0.61 Å to 0.81 Å indicating the variations in the binding site regions of ADP. Likewise, RMSD of ADP bound and unbound

subunit of F1- ATPase (Table 7) reveals the differences in the structural fold in the active site and its coordination with ADP indicating the variations in the bound and unbound form.

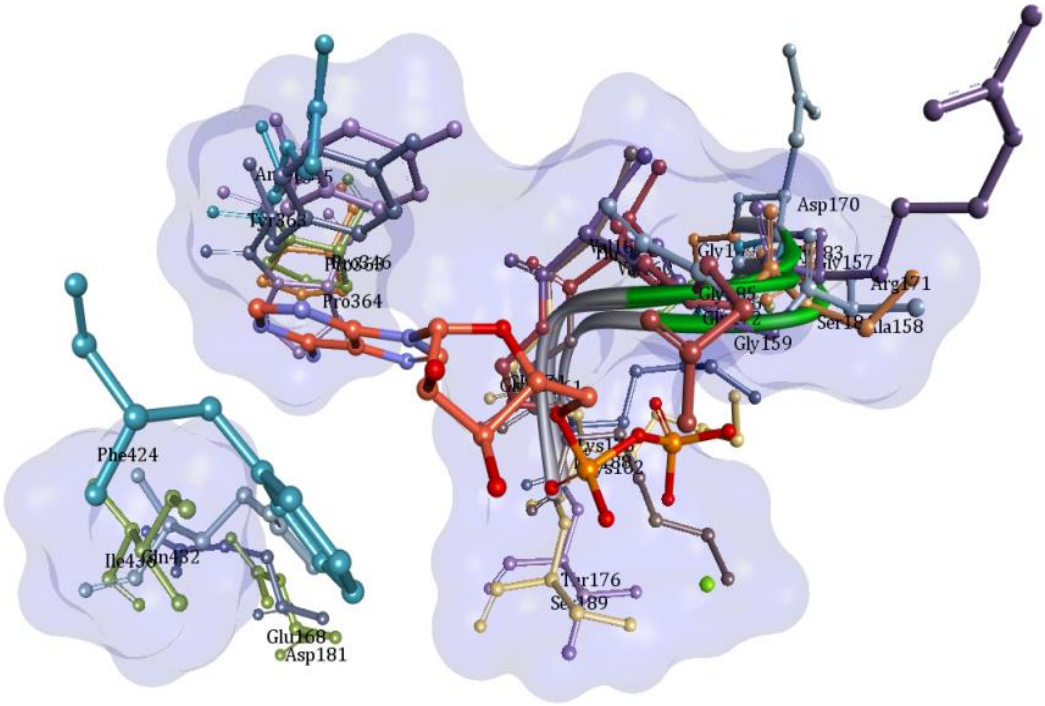

Figure 4: Active site residues overlay showing the conserved residues through FliI-A chain and F1-ATPase α Subunit and β Subunit.

Table 5: Displaying R.M.S.D. values refer to the superposition between F1- ATPase α chain and β chain and between F1- ATPase and FliI chains by the superposition.

RMSD - between F1- ATPase α chain and β chain						
F1- ATPse	1 αA	2 αB	3 αC	1 βD	2 βE	3 β F
1 α A	-	427/0.70 Å	473/1.02 Å	316/1.69 Å	312/1.65 Å	312/1.65 Å
2α B	-	-	465/0.97 Å	304/1.65 Å	298/1.79 Å	298/1.56 Å
3αC	-	-	-	313/1.58 Å	316/1.53 Å	310/1.66 Å
1 β D	-	-	-	-	465/0.59 Å	465/0.59
2 β E	-	-	-	-	-	466/0.00
3 β F	-	-	-	-	-	-
	RMSD of Cα – atoms- range form 0.70-1.02 Å			RMSD of Cα - atoms range form 1.41-1.51 Å		

RMSD between F1- ATPase and FliI- A-chain							
F1- ATPse Chains		1αA	2αB	3α C	1β D	2β E	3βF
FLiI A- A chain	C alpha atoms/ RMSD	335/1.41 Å	295/1.40 Å	320/1.51 Å	269/1.78 Å	266/1.70 Å	266/1.70 Å
	Side chain atoms/ RMSD	1348/1.41 Å	1180/1.40 Å	1252/1.53 Å	1080/1.79 Å	1060/1.71 Å	1060/1.71 Å
		RMSD of Cα – atoms- range form 1.40-1.53 Å			RMSD of Cα – atoms- range form 1.70-1.78 Å		

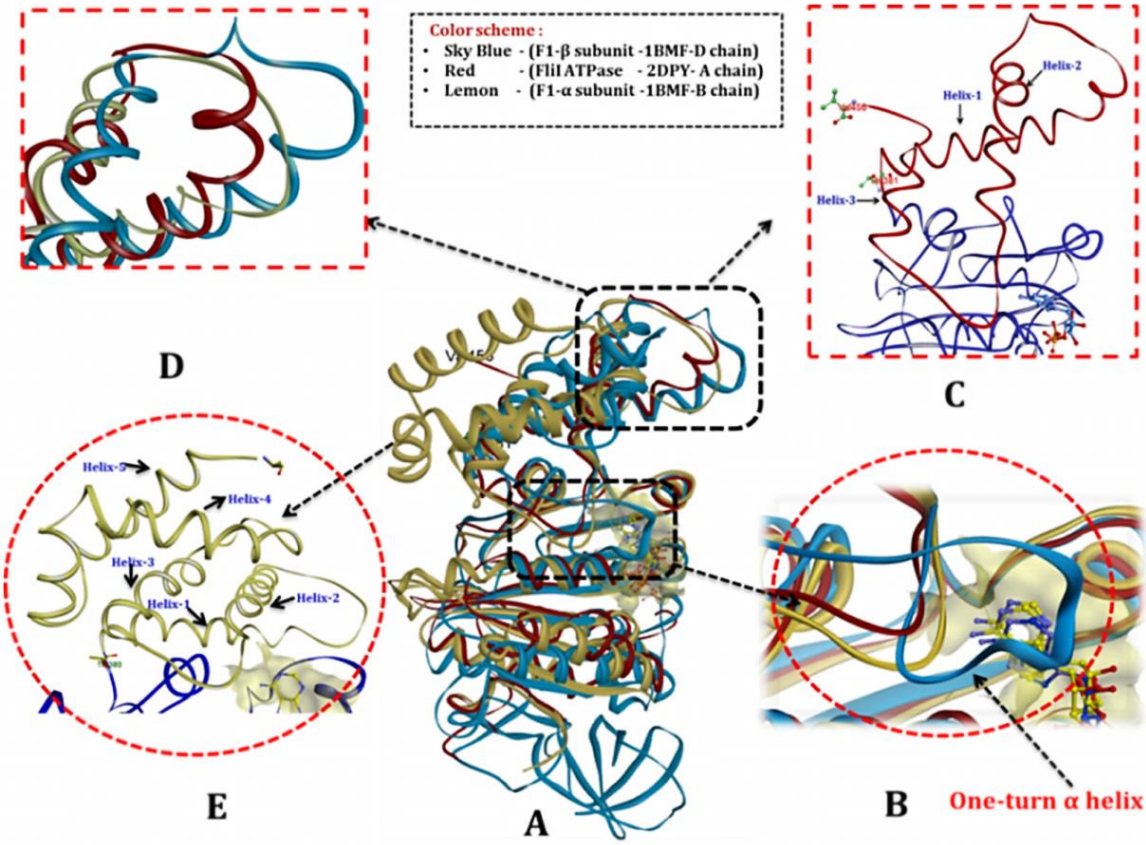

Figure 5: Structural comparison of the FliI [PDB ID- 2DPY] and bovine mitochondrial F1-ATPase (PDBID-1BMF). A] F1-ATPase, α Subunit (Lemon Yellow), β Subunit (Sky Blue) is superimposed onto FliI (Red). B] Figure showing one-turn α helix (Sky blue) which is Specific to β Subunit of F1-ATPase at the ATP binding site. C] Small C-Terminal Domain of FliI showing three Helices. D] Variations in Helical turn/loop between three different chains. E] C- terminal Domain Helices of F1-ATPase Subunits.

Table 6: Displaying r.m.s.d. values Active site residues overlay F1- ATPase α chain and β chain and between F1- ATPase and FliI-A chain.

	RMSD - Active site residues of F1- ATPase α chain and β chain and FliI-A chain			
		F1- ATPse α B	F1- ATPse β D	FLiI - A chain
F1- ATPse α B	C alpha atoms/ RMSD	-	12* /0.46 Å	12*/0.81 Å
	All atoms / RMSD	-	40/0.61 Å	44*/0.81 Å
F1- ATPse β D	C alpha atoms/ RMSD	-	-	12/1.71 Å
	All atoms / RMSD	-	-	40/0.61 Å
FLiI - A chain	C alpha atoms/ RMSD	-	-	-
	All atoms / RMSD			

Table 7: Showing R.M.S.D. values Between ADP Bound and Unbound chains of F1- ATPase Subunits

RMSD - between ADP bound and Unbound chains of F1- ATPase	
C alpha atoms/RMSD	290/1.59 Å
Side chain atoms/ RMSD	828/1.93 Å
All atoms / RMSD	1008/1.85 Å

Similarly, systematic analysis of different secondary structural elements (α helices), Domains and Nucleotide binding sites between FliI-ATPase (A-chain) and bovine mitochondrial F1- ATPase (αA and βD chains) exhibited significant dissimilarity. The FliI C-terminal domain found smaller than the F1- ATPase C domain, involving 3 Helices (Helix1, Helix2 and Helix3) and all these helices structurally share with those of F1-ATPase domain [Figure 5-A-C]. However, C terminal domain of F1-ATPase contains 5 alpha Helices. The F1-β subunit C- domain shows the presence of one-turn α helix between the C2 and C3 α helices. (Figure-5B). However, this is found missing in FliI-C subunit. The details of all Helices are shown in the figure–5 E. Structurally this one-turn α helix appears to assist in making the hydrophobic pocket for the adenine ring deep and providing more region for ATP in F1-β subunit C- domain, while, in FliI ATP-binding site is comparatively shallow, just similar to that of the F1-α subunit. Whereas, Overlay, of the F1-α/β subunits show different conformations depending on the nucleotide-binding state by changing the relative orientation of the ATPase and C-terminal domains.

3.3. Docking Studies with Natural Compounds and Antibiotics

The *In silico* docking results for the natural compounds inhibitors complex are shown in the Figure 6, with the FliI active site and the coordinates of ADP bound to the same site for comparison. The docking poses reveal that, orientation of the FliI protein in each of the docked ligand Poses, as well as that of ADP, differs slightly from one pose view to the next. Observation from the figure 6 and table 8 reveals that the all the compounds occupy the active-site cleft in a similar manner and essentially the entire active-site cleft, including the p-loop region (179–185). While, Lys 188 main conserved residue in most of the ATPases is required for the ATPase activity. Likewise, they also bind across hydrophobic pocket involving Glu-211, Arg-212, Glu-215 and ASP-218, which are expected to be involved in $Mg2^{+}$ and the Phosphate binding. Similarly, Prodiogiosin Exhibit Strong Binding across Adenine binding Hydrophobic Pocket with residues Tyr-363, Pro-364, and Ile-436. Docked compounds across the ADP site; shows that 4 compounds, Vanillin, Safrole, Prodiogiosin & Cucurbitacin show strong binding affinity and with lowest energy ligand-complexes scoring function (-12 to-16 kcal/mol). All molecules exhibit good interactions with 3 to 6 hydrogen bonds within 5.5Å, with good binding energies. Details of Amino acids interacting and binding energies are shown in table 10. The docked molecular interactions across the active site is exhibit similar among the molecules. These docking results also disclose that, the inhibitor conformations and their orientations within the active-site cleft not only sterically hamper the ATP substrate from occupying the active-site cleft; they also obstruct the formation of non-covalent interactions and hydrogen bonding between the substrate and the FliI protein activity. The antibiotics were also chosen along with natural compounds for the docking studies to understand and compare the binding affinity, energy with ADP site and to appreciate the similar affinity with natural compounds compared to antibiotics. Docking results were highlighted in the

table 6. The data from table indicate that, natural compounds also exhibit similar binding affinities indicating that, these can be used as therapeutic targets than antibiotics.

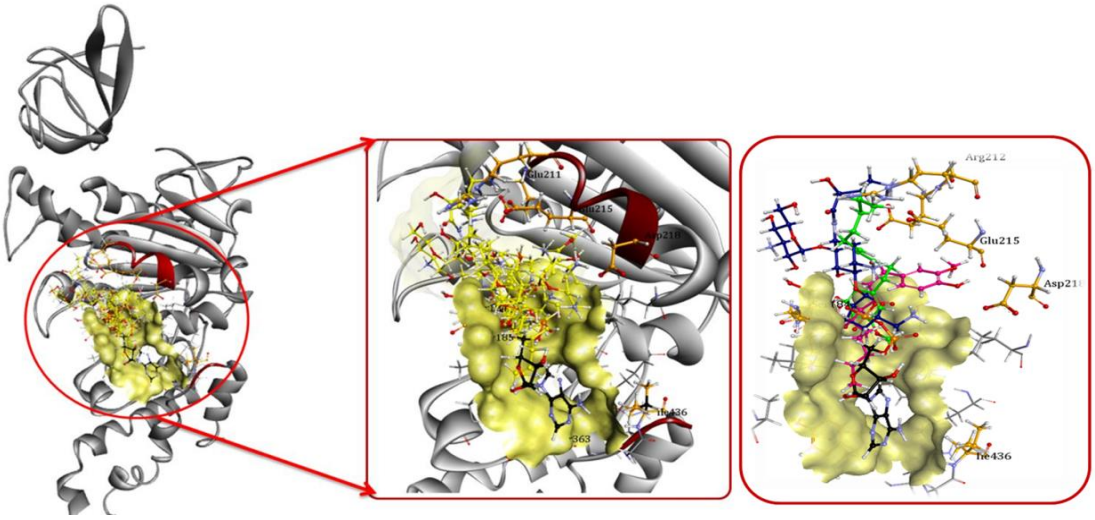

Figure 6: A) Docking results of FliI with ADP and various inhibitor compounds. b) Showing the key residue interactions and Comparison of the docking complexes of ADP with Shogaol (green), Gingerol (Magnata) Amikacin (Navy Blue).

Table 8: Tables showing the compounds used of docking analysis

Sl. No	NATURAL COMPOUND	STRUCTURE	MOLECULAR FORMULA	MOLECULAR WEIGHT(G/MOL)	PUB CHEM CID/SOLUBILITY	SOURCE/ACTION
1	**Vanillin**	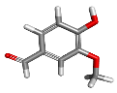	$C_8H_8O_3$	**152.14732**	1183 (hydrophilic)	Constituent in various tissues of several plant species. Vanillin occurs in a wide variety of foods and plants such as orchids; major commercial source of natural vanillin is from vanilla bean extract
2	**Carvacrol**	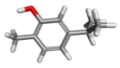	$C_{10}H_{14}O$	**150.21756**	10364 (lipophilic compound)	Found in oil of origanum, thyme, marjoram, summer savory.
3	**ShogÅl**		$C_{17}H_{24}O_3$	**276.37066**	5281794 (lipophilic compound)	Found in oil of origanum, thyme, marjoram, summer savory.
4	**Safrole**	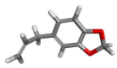	$C_{10}H_{10}O_2$	**162.1852**	5144 (lipophilic compound)	Found in oil of origanum, thyme, marjoram, summer savory.
5	**6-Gingerol**	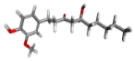	**C17H26O4**	**294.38594**	442793 (lipophilic compound)	Bioactive Compound Found In Raw Ginger (Zingiber Officinale) With Antioxidant Activity
6	**D-Piperitone**	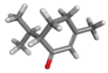	$C_{10}H_{16}O$	**152.23344**	61362 (hydrophilic)	Component of some essential oils and Eucalyptus dives
7	**Eugenol**	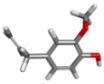	$C_{10}H_{12}O_2$	**164.20108**	3314 (hydrophilic)	Main component of several essential oils; clove leaf oil and cinnamon leaf oil.
8	**PRODIGIOSIN**		$C_{20}H_{25}N_3O$	**323.432**	**5351169** (hydrophilic)	Prodigiosin is a tripyrrole red pigment secondary metabolite biosynthesized by *Serratia marcescens* and other bacteria
9	**Cucurbitacin**		$C_{32}H_{46}O_8$	**5281316**	558.70284 (lipophilic compound)	Cucurbitacin is any of a class of biochemical compounds that some plants — notably members of the family cucurbitaceae,

Docking studies also specify the existence of additional binding sites across the N-Terminal region of FliI that can also lodge the these small natural molecules that can hindering the its function. Therefore, through our Insilco studies we propose the use of these compounds as effective inhibitors of FliI ATPase, whose main function is in the export of flagellar proteins through its central channel. If these inhibitors can effectively halt the oligomerization of FliI into homohexamer in vitro, then translocation of many flagella proteins it is hampered and the movement of the bacteria towards the target organs is hindered. From the sequence and structural alignment results specify that the, FliI ATPase's are also show structural similarity with YscN, Therefore, our study also extended to know the binding interactions of these compound across Injectisome ATPase homolog YscN, as an off-target protein. Docking studies with YscN also revealed the similar substantial results, indicating usage of these natural compounds as the possible therapeutic molecules. Our novel interest was also extended in understanding the binding interaction with all other remaining 16 flagellar structural proteins involved in the flagellar movement. Comprehensive structural, binding pocket and docking analysis was carried out against the active sites of the proteins. Results of molecular docking were highlighted in the Table.9 indicating the binding energies and the strength of interactions with the Ligands and Antibiotics. As a result, the effective inhibitors of the specific proteins can block the formation of flagellum and also the motility of bacteria. This study focuses on the importance of FLiI ATPase as the most important component of the export apparatus system and further *in vivo* studies need to be carried out to determine the effectiveness of the ligands considered for the present study.

Table 9: Tables showing the Antibiotics used of docking analysis

SL NO	ANTIBIOTICS	STRUCTURE	MOLECULAR FORMULA	MOLECULAR WEIGHT(G/MOL)	PUB CHEM CID	SOURCE/ACTION
1	NETILMICIN	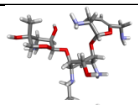	$C_{21}H_{41}N_5O_7$	475.57954	441306	Netilmicin is an aminoglycoside antibacterial. The chemical classification of netilmicin is aminoglycosides.
2	ACRIFLAVIN	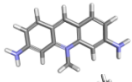	$C_{14}H_{14}N_3^+$	224.28106	2016	Acriflavine is a topical antiseptic.
3	AMIKACIN	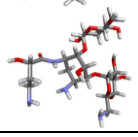	C22H43N5O13	585.60252	37768	Amikacin base is a broad-spectrum semi-synthetic aminoglycoside antibiotic

Table 10: Docking results Tables showing the Antibiotics used of docking analysis

FLAGELLAR PROTEIN	NATURAL COMPOUNDS								ANTIBIOTICS			
PROTEIN/ PDBID	VANILLIN	CARVACROL	SHOGÅL	SAFROLE	GINGEROL	EUGENOL	PRODIOGIOSIN	CUCURBITACIN	NETILMICIN	ACRIFLAVIN	AMIKACIN	NO OF ENERGY >10
FliI-2DPY	GLY-183 SER189 GLY-187 VAL-186 SER-189 LYS-188	GLY-183 VAL-186 LYS-188	GLY-183 LYS-188 SER-189	GLY-185 LYS-188 VAL-186 GLY-187 SER-189	GLY-183 LYS-188 SER-189 ARG-212 GLU-215	GLY-183 LYS-188 SER-189	GLY183 VAL190 ARG-212 GLU-215 TYR-363 PRO 364 TLE436	GLY-183 LYS-188 GLY-187 SER-189 VAL-186	GLY-183 SER-189 GLU-215 ASP-218 GLU-211	GLY-183 ASP-218 GLU-215	GLU-331 GLY- 210 GLU-211 GLU-215 GLY-183 VAL-186 GLY-187 SER-189	
Hydrophobic interactions	SER-184 GLY-185	GLY-185 SER-189 SER-184 ARG-212 GLU-215 LEU-329	ARG-212 GLU-215 SER-184 LYS-188 GLU-211		GLY-185	GLY-185 LEU-329 SER-184		GLY-187 SER-184 SER-189 LYS-188	ILE-239 VAL-186 LYS-188 GLY-187 SER-184 SER-189 LYS-188	LYS-188 SER-189 VAL-186 GLU-211 ILE-223	SER-184 LEU-329	
Binding energy in Å kcal/mol	-15.1709	-13.0769	-10.4735	-15.0091	-12.6674	-11.4972	-16.9046	-15.7387	-17.2361	-12.5478	-13.2586	(09)03

Table 11: Docking analysis Table showing the strength of interactions with the Ligand and Antibiotics used of docking analysis

	FLAGELLAR PROTEINS		NATURAL COMPOUNDS								ANTIBIOTICS			
Sl No	PROTEIN/PDBID	FUNCTION/PROPERTIES OCCURRENCE IN FLAGELLA	VANILLIN	CARVACROL	SHOGAL	SAFROLE	GINGEROL	EUGENOL	PRODIOGISIN	CUCURBITACIN	NETILMICIN	ACRIFLAVIN	AMIKACIN	NO OF ENERGY >10
1	FlgL-2D4X	Flagellar hook-associated protein 3(Hook)	**-8.5672**	-8.0822	-4.9894	-7.9917	-7.5848	-6.3935	-12.3620	-8.5672	-17.5443	-13.1871	-12.7866	**02(02)**
2	FliK-2RRL	**Flagellar hook-length control protein(Hook)**	**-13.4688**	-12.4200	7.6011	-10.6962	-8.3402	-10.1251	-13.2712	-13.4688	-12.1762	-18.6833	-2.2209	**(04)04**
3	FliI-2DPY	**Flagellum-specific ATP synthase (Cytoplasm)**	**-15.1709**	**-13.0769**	-10.4735	**-15.0091**	**-12.6674**	-11.4972	-16.9046	-15.7387	-17.2361	-12.5478	-13.2586	**(09)03**
4	FlhD-1G8E	**Flagellar transcriptional (Cytoplasm)**	**-11.0049**	-6.5348	**-7.1812**	-5.7925	-7.8166	**-8.3903**	-15.6112	-11.0049	-18.8867	-15.6587	-7.1797	**(o2)03**
5	FlhB-3B0Z	**Flagellar biosynthetic protein FlhB (Cytoplasm)**	-8.4234	-7.8965	-6.2117	-6.6678	-3.6701	-6.6227	-5.2679	-8.4234	-13.044	-13.9620	-10.2772	**(01) 02**
6	FlgA-3TEE	Flagella basal body P-ring formation protein (basal Body)	**-15.6889**	-10.4102	-11.2389	-8.3299	**-12.0196**	**-11.7873**	-12.8686	-15.6889	-12.5077	-14.2269	-10.7803	**(05)03**
7	FlhA-3A5I	Flagellar biosynthesis protein FlhA(Cytoplasm)	-11.1451	-7.9016	-14.0863	-8.2225	-11.0051	-9.0011	-13.2091	-11.1451	-16.2391	-14.9652	-12.8018	**(04)04**
8	FlgK-2D4Y	Flagellar hook-associated protein 1 (Hook)	**-15.3257**	-8.4927	**-11.4487**	-9.3280	-11.9156	**-9.8627**	-14.2694	-15.3257	-26.2867	-18.4320	-23.4888	**(05)03**
9	FliS-3IQC	Flagellar protein (Cytoplasm)	**-8.2905**	**-7.7161**	-5.2306	**-7.3700**	-3.2338	-4.6715	-13.6012	*-8.2905*	-15.7914	-13.9042	-2.2452	**(02)01**
10	FliM-4GC8	Flagellar motor switch protein(Cytoplasm C ring)	**-12.2659**	-9.2484	**-12.0749**	-10.3701	**-11.8433**	-10.0293	-10.1289	-12.2659	-14.4981	-12.8880	-6.2396	**(07)02**
11	FliJ-3AJW	**Flagellar FliJ protein (Cytoplasm)**	-9.8504	-10.7066	-4.3216	-6.2154	-9.8504	-5.7278	-14.2547	-9.8504	-11.3367	-12.3817	-1.0706	**(03)01**
12	FliT-3A7M	Flagellar protein (Cytoplasm)	**-10.8646**	-10.8646	-4.4757	-6.8142	-7.2351	-8.0289	-12.5879	-10.8646	-9.9270	-13.8495	-0.0272	**(04) 01**
13	FliG-3USW	Flagellar motor switch protein (Rotor)	**-16.1890**	-9.2272	**-12.4806**	-10.3121	**-12.2884**	-10.0164	-14.8468	-16.1890	-16.3228	-13.4075	-15.7376	**(07)03**
14	FlgE-1WLG	Flagellar hook protein (Hook)	**-10.4142**	**-8.3270**	-6.8291	**-8.6546**	6.4918	-6.6929	-11.4714	-10.4142	-10.3269	-15.1064	-6.3183	**(03) 02**
15	MotB-3SOY	Motility protein (cytoplasmic membrane)	**-12.6177**	**-10.8201**	-9.4182	-8.6873	**-10.2369**	-10.9220	-14.7156	-12.6177	12.0187	-16.7589	-1.5087	**(05) 02**
16	FlgD-3OSV	Flagellar basal-body rod modification protein (basal Body)	**-12.6562**	**-8.0235**	-7.9627	**-8.7899**	-8.2895	-6.3684	-9.5626	-12.6562	12.4036	-13.6123	-15.2526	**(01)04**
17	CheY-4HNS	CheY homolog	**-10.7359**	**-10.0316**	**-8.2172**	-8.5950	-19.0250	8.8658	-9.6692	10.7359	19.6609	-12.1195	-11.1119	**(04) 03**
	Strength of Binding (>-)10		**12**	**06**	**06**	**04**	**05**	**06**	**14**	**13**	**16**	**17**	**10**	

DISCUSSION

As the rise of antibiotic resistance coincides with a shortage of unique drugs and also need for novel antibiotics that do not promote the rapid evolution of resistance, there is need for development of these anti-virulence compounds. The emerging threat of multidrug-resistant bacteria has led researchers to discover virulence blockers as novel classes of antibiotics. However, this is a difficult goal that requires the more economic resources for antibiotic research. Much research has focused on inhibitors of the T3SS, which is appropriate given the lack of new antibiotics in development to combat Gram-negative infection and the ubiquity of T3SSs in Gram-negative pathogens. Therefore, Search for Natural compounds can help in curing the pathogenicity and virulence. The data from our results establish the probability of targeting and inhibiting a critical protein transport ATPase of a bacterial virulence system. It is likely the same strategy could be applied to many other common human pathogens using type III secretion system, *In silico* methods was used to determine the conformations of natural compounds when bound to the active site of FliI and YscN. In each case, the compounds were shown to bind the FliI protein within or in close proximity to its active site [Figure 5]. Our goal was to determine and study the three-dimensional structures of the respective compound– ATPase complexes to initiate the design of natural compounds that could be used as lead compounds in the development of high-potency, broad-spectrum therapeutics against T3SS pathogens by inhibiting the faleklar motion and virulence across Injectisome ATPase's. Since ATPases are difficult to crystallize, and efforts to crystallize T3SS ATPases have not been successful to date. Moreover, as shown by *In silico* results [Figure 5, Table 5 and 6], these compounds could occupy the FliI and YscN active site in a alike mode [Figure 4]. In addition, all compounds occupy the active site in a manner similar to ADP in the FliI. Therefore, it is sensible to accept that most of the compounds occupy the site in a manner similar to that of the ATP substrate as well and obstruct ATP substrate binding. Of the selected natural compounds studied, compounds like Vanillin, Carvacrol, Safrole, Gingerol, Prodiogiosin Cucurbitacin displayed the probable drug like candidates in the development of broad-spectrum therapeutics. It is interesting to note that they also bind to the N terminal region showing the probable deactivation of FliI. As the rise of antibiotic resistance coincides with a shortage of unique drugs and also need for novel antibiotics that do not promote the rapid evolution of resistance, there is need for development of these anti-virulence compounds. The emerging threat of multidrug-resistant bacteria has led researchers to discover virulence blockers as novel classes of antibiotics. However, this is a difficult goal that requires the more economic resources for antibiotic research. Much research has focused on inhibitors of the T3SS, which is appropriate given the lack of new antibiotics in development to combat Gram-negative infection and the ubiquity of T3SSs in Gram-negative pathogens. Therefore, Search for Natural compounds can help in curing the pathogenicity and virulence.

4. CONCLUSION

The data from our results establish the probability of targeting and inhibiting a critical protein transport ATPase of a bacterial virulence system. It is likely the same strategy could be applied to many other common human pathogens using type III secretion system, *In silico* methods was used to determine the conformations of natural compounds when bound to the active site of FliI and YscN. In each case, the compounds were shown to bind the FliI protein within or in close proximity to its active site. (Figure 5). Our goal was to determine and study the three-dimensional structures of the respective compound– ATPase complexes to initiate the design of natural compounds that could be used as lead compounds in the development of high-potency, broad-spectrum therapeutics against T3SS pathogens by inhibiting the faleklar motion and virulence across Injectisome ATPase's. Since ATPases are difficult to crystallize, and efforts to crystallize T3SS ATPases have not been successful to date. Moreover, as shown by *In silico* results [Figures 5, Table 5 and 6], these compounds could occupy the FliI and YscN active site in a alike mode [Figure 5]. In addition, all compounds occupy the active site in a manner similar to ADP in the FliI. Therefore, it is sensible to accept that most of the compounds occupy the site in a manner similar to that of the ATP substrate as well and obstruct ATP substrate binding. Of the selected natural compounds studied, compounds like Vanillin, Carvacrol, Safrole, Gingerol, Prodiogiosin Cucurbitacin displayed the probable drug like candidates in the development of broad-spectrum therapeutics. It is interesting to note that they also bind to the N terminal region showing the probable deactivation of F FliI.

ACKNOWLEDGEMENT

The authors gratefully acknowledge the generous support and facilities extended by Sir M. Visvesvarya Institute of Technology and Sri Krishnadevaraya Educational Trust, Bangalore, towards this project.

CONFLICT OF INTEREST

Authors have no conflict of interest.

REFERENCES

1. Imada K, Minamino T, Tahara A, Namba K. Structural similarity between the flagellar type III ATPase FliI and F1-ATPase subunits. Proc Natl Acad Sci USA. 2007;104(2):485-90.
2. Ibuki T, Imada K, Minamino T, Kato T, Miyata T, Namba K. Common architecture of the flagellar type III protein export apparatus and F- and V-type ATPases. Nat Struct Mol Biol. 2011 Mar;18(3):277-82.
3. Imada K, Minamino T, Uchida Y, Kinoshita M, Namba K. Insight into the flagella type III export revealed by the complex structure of the type III ATPase and its regulator. Proc Natl Acad Sci U S A. 2016 Mar 29;113(13):3633-8.
4. Minamino T, Tame JR, Namba K, Macnab RM. Proteolytic analysis of the FliH/FliI complex, the ATPase component of the type III flagellar export apparatus of Salmonella. J Mol Biol. 2001

Oct 5;312(5):1027-36.

5. Macnab RM. Type III flagellar protein export and flagellar assembly. Biochim Biophys Acta. 2004;1694(1-3):207-17.
6. Minamino T, Macnab RM. Components of the Salmonella flagellar export apparatus and classification of export substrates. J Bacteriol. 1999 Mar;181(5):1388-94.
7. III secretion. Nature. 2008 Jan 24;451(7177):489-92.
8. Common and distinct structural features of Salmonella injectisome and flagellar basal body. Sci Rep. 2013 Nov 28;3:3369.
9. Gao B, Lara-tejero M, Lefebre M, Goodman AL, Galán JE. Novel components of the flagellar system in epsilonproteobacteria. M Bio. 2014;5(3):e01349-14.
10. Gophna U, Ron EZ, Graur D 2003. Bacterial type III secretion systems are ancient and evolved by multiple horizontal-transfer events. Gene 312: 151–163
11. Notti RQ, Stebbins CE. The Structure and Function of Type III Secretion Systems. Microbiol Spectr. 2016;4(1)
12. Minamino T, Imada K, Namba K. Mechanisms of type III protein export for bacterial flagellar assembly. Mol Biosyst. 2008;4(11):1105-15.
13. Hueck CJ. Type III protein secretion systems in bacterial pathogens of animals and plants. Microbiol Mol Biol Rev. 1998 Jun; 62(2):379-433.
14. Claret L, Calder SR, Higgins M, Hughes C. Oligomerization and activation of the FliI ATPase central to bacterial flagellum assembly. Mol Microbiol. 2003;48(5):1349-55
15. Fan F, Macnab RM. Enzymatic characterization of FliI. An ATPase involved in flagellar assembly in Salmonella typhimurium. J Biol Chem. 1996;271(50):31981-8.
16. Auvray F, Ozin AJ, Claret L, Hughes C. Intrinsic membrane targeting of the flagellar export ATPase FliI: interaction with acidic phospholipids and FliH. J Mol Biol. 2002;318(4):941-50.
17. Haiko J, Westerlund-wikström B. The role of the bacterial flagellum in adhesion and virulence. Biology (Basel). 2013;2(4):1242-67.
18. Butler SM, Camilli A. Going against the grain: chemotaxis and infection in Vibrio cholerae. Nat Rev Microbiol. 2005;3(8):611-20.
19. Ibuki T, Imada K, Minamino T, Kato T, Miyata T, Namba K. Common architecture of the flagellar type III protein export apparatus and F- and V-type ATPases. Nat Struct Mol Biol. 2011;18(3):277-82.
20. A Evans LD, Stafford GP, Ahmed S, Fraser GM, Hughes C. An escort mechanism for cycling of export chaperones during flagellum assembly. Proc Natl Acad Sci U S A. 2006 Nov 14;103(46):17474-9.

21. Stafford GP, Evans LD, Krumscheid R, Dhillon P, Fraser GM, Hughes C. Sorting of early and late flagellar subunits after docking at the membrane ATPase of the type III export pathway. J Mol Biol. 2007 Dec 7;374(4):877-82.
22. Lane MC, O'Toole PW, Moore SA. Molecular basis of the interaction between the flagellar export proteins FliI and FliH from Helicobacter pylori. J Biol Chem. 2006 Jan 6;281(1):508-17.
23. Cornelis GR. The type III secretion injectisome. Nat Rev Microbiol. 2006;4(11):811-25.
24. Blaylock B, Riordan KE, Missiakas DM, Schneewind O. Characterization of theYersinia enterocolitica type III secretion ATPase YscN and its regulator, YscL. JBacteriol. 2006 May;188(10):3525-34.
25. https://www.ncbi.nlm.nih.gov/pubmed/
26. The Universal Protein Resource (UniProt). Nucleic Acids Res. 2007;35(Database issue): D193-7.
27. Berman HM, Westbrook J, Feng Z, et al. The Protein Data Bank. Nucleic Acids Res. 2000; 28(1):235-42.
28. Kim S, Thiessen PA, Bolton EE, et al. PubChem Substance and Compound databases. Nucleic Acids Res. 2016;44(D1):D1202-13.
29. Kramer B, Rarey M, Lengauer T. Evaluation of the FLEXX incremental construction algorithm for protein-ligand docking. Proteins. 1999; 37 (2):228-41.
30. Koska J, Spassov VZ, Maynard AJ, et al. Fully automated molecular mechanics based induced fit protein-ligand docking method. J Chem Inf Model. 2008;48 (10):1965-73.